UNIVERSITY
OF WOLLONGONG
AUSTRALIA

University of Wollongong
Research Online

Faculty of Science - Papers (Archive)

Faculty of Science, Medicine and Health

2012

Luminescence dating of Chinese loess beyond 130 ka using the non-fading signal from K-feldspar

Bo Li
University of Wollongong, bli@uow.edu.au

Shenghua Li
University of Hong Kong

Publication Details

Li, B. & Li, S. (2012). Luminescence dating of Chinese loess beyond 130 ka using the non-fading signal from K-feldspar. Quaternary Geochronology, 10 24-31.

Research Online is the open access institutional repository for the University of Wollongong. For further information contact the UOW Library: research-pubs@uow.edu.au

Luminescence dating of Chinese loess beyond 130 ka using the non-fading signal from K-feldspar

Abstract
A multi-elevated-temperature post-IR IRSL (MET-pIRIR) protocol, which utilizes the IRSL signals measured by progressively increasing the stimulation temperature from 50 to 300 °C in a step of 50 °C, was applied to date the potassium-rich feldspar (K-feldspar) extracts from loess samples at the Luochuan section of the Chinese Loess Plateau. It was observed that the MET-pIRIR ages obtained at elevatedtemperatures (250 and 300 °C) are consistent with independent chronological control for the samples from the first loess layer (L1) to the third paleosol layer (S3), which correspond to the marine isotope stages (MIS) 2e9. Our results indicate that the MET-pIRIR protocol can provide reliable ages for the Chinese loess up to ~300 ka. The results suggest that the MET-pIRIR signal measured at 250 and 300 °C gives the most reliable ages for older samples (>130 ka). For samples below L3, the natural MET-pIRIR signals measured at high temperatures reach the saturation level in dose response curves, suggesting a dating limit of ~300 ka for the Luochuan loess section.

Keywords
luminescence, signal, fading, non, ka, 130, feldspar, beyond, k, loess, chinese, dating, CAS

Disciplines
Life Sciences | Physical Sciences and Mathematics | Social and Behavioral Sciences

Publication Details
Li, B. & Li, S. (2012). Luminescence dating of Chinese loess beyond 130 ka using the non-fading signal from K-feldspar. Quaternary Geochronology, 10 24-31.

This journal article is available at Research Online: http://ro.uow.edu.au/scipapers/4437

Luminescence dating of Chinese Loess beyond 130 ka using the non-fading signal from K-feldspar

Bo Li [a,b,*], Sheng-Hua Li [a]

a Department of Earth Sciences, The University of Hong Kong, Pokfulam Road, Hong Kong, China

b Centre for Archaeological Science, School of Earth & Environmental Sciences, The University of Wollongong, Wollongong, NSW 2522, Australia*Corresponding author: Email: boli@hku.hk, Fax: +852-25176912

Abstract

A multi-elevated-temperature post-IR IRSL (MET-pIRIR) protocol, which utilizes the IRSL signals measured by progressively increasing the stimulation temperature from 50 to 300°C in a step of 50°C, has been applied to date the potassium-rich feldspar (K-feldspar) extracts from loess samples at the Luochuan section of the Chinese Loess Plateau. It was observed that the MET-pIRIR ages obtained at elevated temperatures (250 and 300 °C) are consistent with independent chronological control for the samples from the first loess layer (L1) to the third paleosol layer (S3), which correspond to the marine isotope stages (MIS) 2 to 8. Our results indicate that the MET-pIRIR protocol can provide reliable ages for the Chinese loess up to ~300 ka. The results suggest that, for young samples (<130 ka), it is preferable to use the MET-pIRIR signal at 200°C due to its low residual age. However, the MET-pIRIR signal measured at 250 and 300 °C gives the most reliable ages for older samples (>130 ka). For samples below L3, the natural MET-pIRIR signals measured at high temperatures reach the saturation level in dose response curves, suggesting a dating limit of ~300 ka for the Luochuan loess section.

Keywords: K-feldspar, luminescence dating, post-IR IRSL, Luochuan loess.

1. Introduction

Chinese loess provides an ideal profile of past climatic change, due to its quasi-continuous nature of dust deposition (Liu, 1985). Luminescence dating is one of the main tools for dating loess, and it has been extensively applied to loess sections in China in the last three decades (Forman, 1991; Frechen, 1999; Lai et al., 2010; Lu et al., 1987; Wang et al., 2006; Zhou and Shackleton, 2001). However, most of these studies were limited to the upper most loess and paleosol sections (S0, L1 and S1) (Buylaert et al., 2007; Lai, 2010; Lu et al., 2007). Optical stimulated luminescence (OSL) dating of Chinese loess beyond ~130 ka has long been a challenge for luminescence researchers, mainly due to the early saturation of quartz OSL signal.

Feldspar is a promising candidate for extending the luminescence dating limit due to its much higher saturation dose. However, the anomalous fading of the infrared stimulated luminescence (IRSL) signal from feldspar has hampered the application of feldspar in optical dating (e.g. Huntley and Lamothe, 2001; Huntley and Lian, 2006; Lamothe and Auclair, 1999; Li et al., 2007). Recent progresses in understanding the anomalous fading of the IRSL from feldspar have allowed the possibility of isolation of a non-fading component in feldspar IRSL. It has been suggested that the initial part of the IRSL signal has a higher anomalous fading rate when compared to the later part (Thomsen et al., 2008). This observation has led to the development of a post-IR IRSL dating method, in which an IRSL bleaching at low temperature (~50°C) is applied before a high temperature (>200°C) IRSL measurement to reduce the fading rate of feldspar (Thomsen et al., 2008; Buylaert et al., 2009; Thiel et al., 2011). It was suggested that, when a high-temperature post-IR IRSL (pIRIR) was conducted at 290 °C, it is possible to obtain a non-fading signal (Thiel et al., 2011). However, detectable anomalous fading is still present in the elevated-temperature post-IR IRSL signals (Buylaert et al., 2009), although Thiel et al. (2011) suggested that fading correction is not necessary for their samples.

More recently, Li and Li (2011) found that a multiple IR stimulation procedure with increasing stimulation temperature is able to isolate the non-fading IRSL signal. Based on this observation, a

protocol for IRSL dating K-rich feldspar has been proposed, which utilizes the IRSL signals measured by progressively increasing the stimulation temperature from 50 to 250°C in a step of 50°C, and is called multi-elevated-temperature post-IR IRSL (MET-pIRIR) protocol (Li and Li, 2011). The laboratory fading test for a feldspar sample showed that there are negligible anomalous fading rates (g values) for the MET-pIRIR signals obtained at 200°C and 250°C. Hence, no fading correction is required. The reliability of this protocol has been tested using various sedimentary samples from China deposited in the last ~130 ka (Li and Li, 2011). It was observed that the MET-pIRIR ages obtained at 200 and 250 °C are consistent with independent or quartz OSL ages.

In this study, we further tested the MET-pIRIR applicability to potassium-rich feldspar (K-feldspar) extracts from loess samples from the Luochuan section of the Chinese Loess Plateau. The method was applied to samples from the first loess layer (L1) to the third paleosol layer (S3), corresponding to marine isotope stages from MIS 2 to MIS 9. We aim to test the validity of the MET-pIRIR protocol for loess samples older than 130 ka by comparing with the well-established stratigraphic ages for Chinese loess (Ding et al., 2002). Finally we explore the MET-pIRIR age limit.

2. Luochuan section and samples

The Luochuan section has been extensively studied as one of the well-known sections in the Chinese Loess Plateau for palaeo-environmental studies (An et al., 1991; Liu, 1985; Porter and An, 1995). The chronology of the upper most loess and paleosol (S0, L1 and S1) of this section has been established using the sensitivity-corrected multiple-aliquot regenerative-dose (MAR) OSL dating protocol for quartz (Lu et al., 2007). For the lower part of the section, independent ages can be obtained by climatic correlation to the well-established chronology in the marine sediments reported by Imbrie et al. (1984) (Liu, 1985; An et al., 1991; Porter and An, 1995). Based on orbital tuning of the grain-size records from several sections in Chinese Loess Plateau, Ding et al. (2002) established a stacked climate record of the Quaternary period from the Chinese loess, which can be correlated with the oxygen isotopic record in deep-sea sediments. Here we adopt the ages of the loess/paleosol

boundaries provided by Ding et al. (2002) as an independent age control for our samples, i.e. the age of individual sample can be obtained by linearly interpolating their stratigraphic positions (sampling depth) into the corresponding loess/paleosol boundary ages in which the samples were embedded. A total of 14 samples were collected between the top of first loess layer (L1) to the upper part of the forth loess layer (L4). Another was collected from the ninth loess layer (L9), at 63 m bellow the surface. According to Ding et al. (2002), the upper 14 samples were deposited from 20 to 350 ka ago. The sample taken from L9 was expected to have an age of ~900 ka, which is treated as a field-saturated sample, i.e. we expect that the IRSL signal is not growing any longer and has reached an equilibrium state with the dose rate. A summary of the stratigraphy of the section, sampling positions are shown in Table 1.

3. Experimental procedures and analytical facilities

The samples were routinely treated with HCl and H_2O_2 to remove carbonate and organic matter and dried. After that, 63-90 μm grains were obtained by dry sieving. The K-feldspar grains were then separated using the heavy liquid with a density of 2.58 g/cm^3. The K-feldspar grains were etched using 10% HF for 10 minutes to clean the surface of the grains and also reduce the alpha-irradiated layer around the grain surface. The K-feldspar IRSL measurements were made on an automated Risø TL-DA-15 reader equipped with IR diodes (870Δ40 nm) for stimulation (Bøtter-Jensen et al., 2003). The total IR power delivered to the sample position was ~135mW/cm2 (Bøtter-Jensen et al., 2000). Irradiations were carried out within the reader using a ^{90}Sr/^{90}Y beta source. The IRSL signals were detected using a photomultiplier tube with the stimulated luminescencepassing through a filter pack containing Schott BG-39 and Corning 7-59 filters, which provides a blue transmission window (320-480 nm). Aliquots containing several hundred grains were prepared by mounting the grains in a monolayer on a 9.8 mm diameter aluminum disc with “Silkospay” silicone oil.

The environmental (or external) dose rates were measured using the thick-source alpha counting (TSAC) technique (Aitken, 1985) for determining the contribution from U and Th and X-ray fluorescence (XRF) for the K content. The water contents of 15±5% and 20±5%, similar to those used in previous publications (Lai, 2010; Lu et al., 2007), were used for the loess layers and paleosol layers, respectively. The contribution from cosmic ray was calculated from the burial depth and the latitude and altitude of the samples (Prescott and Hutton, 1994). The internal dose rate for K-feldspar used in age calculation was estimated by assuming K=13±1% and Rb=400±100 ppm (Huntley and Baril, 1997Huntley and Hancock, 2001; Zhao and Li, 2005; Li et al. 2008;). A summary of the dosimetry data for all samples is listed in Table 1.

3. The MET-pIRIR protocol

In the original MET-pIRIR protocol proposed by Li and Li (2011), the IRSL signals of both regenerative and test doses were measured for several times and each measurement was conducted by increasing the stimulation temperature in steps of 50°C, e.g. 50, 100, 150, 200 and 250 °C. Based on this protocol, several equivalent doses and ages can be obtained for different MET-pIRIR signals at different stimulation temperatures. A basic feature of the MET-pIRIR protocol is that one can plot the MET-pIRIR ages with the corresponding IR stimulation temperatures, so-called Age_Temperature (A-T) plot. It was observed that the MET-pIRIR ages were increasing with IR temperature, indicating a lower anomalous fading for the signals measured at higher temperatures. An age plateau was reached above 200 °C (Li and Li, 2011). It was found that such age plateau is consistent with quartz OSL ages and independent ages for their samples, indicating that the non-fading component was depleted by previous IR stimulations at lower temperatures. Therefore, an age plateau in the A-T plot could be used as an indicator for whether a stable or non-fading component has been achieved using the MET-pIRIR procedure.

In this study, we applied a MET-pIRIR protocol introduced by Li and Li (2011) where we added stimulations at 300°C. following the 250°C measurement. We will show that a higher MET-pIRIR stimulation temperature above 250 °C was necessary to achieve an age plateau in the A-T plot for older samples (see next sections for details) and the MET-pIRIR measured at 200°C did not reached the stability observed at higher temperature for older samples. A detailed procedure of the protocol used in this study was shown in Table 2. A preheat at 320°C for 60 s (step 2 and 10) was applied after both regenerative and test doses to avoid significant influence from residual phosphorescence while recording the MET-pIRIR at 300°C (step 8 and 16). The IRSL signals of both regenerative and test doses are measured for several times and each measurement was obtained by increasing the stimulation temperature in steps of 50°C, i.e. 50, 100, 150, 200, 250 and 300 °C (Table 2). At the end of the IRSL measurements for each test dose, a 'hot' IR bleaching at 325°C for 100 s (step 17) is conducted to minimize the residual signal preceding the next measurement cycle.

4. Results

4.1 Laboratory dose response curves

The dose response curves (DRCs) for the MET-pIRIR signals were obtained using the procedure of Table 2. It was found that different samples from this section have nearly identical DRCs. Fig. 1 shows the compiled sensitivity-corrected DRCs for different MET-pIRIR temperatures. These DRCs show a continuous growth of up to 1000 Gy, demonstrating a great potential of feldspars for dating old samples.

In Fig. 1, different DRC shapes were observed for various stimulation temperatures. The 50°C IRSL signal has the highest sensitivity-corrected intensity. The DRCs for the 100, 150 and 200 °C signals are similar, but the 250 and 300 °C signals have lower intensities. These DRCs can be fitted using single exponential saturation functions. The fitting results suggest that the 50 °C IRSL signal saturated at the highest dose level (D_0=402 Gy, where D_0 refers to the characteristic saturation dose). The 100, 150 and 200 °C signals saturated at a lower dose than the 50 °C IRSL did but have a similar

saturation dose level, i.e. D_0=338, 362 and 358 Gy, respectively. Lower saturation doses of 327 and 250 Gy were observed for the 250 and 300 °C signals, respectively.

Routine tests of recycling ratio and recuperation or the ratio between the signal responses of zero dose and natural dose can be conducted in construction of DRCs during D_e measurements (Wintle and Murray, 2006). The recycling ratios for all of the samples fall within the range of 1.0±0.1, and the recuperation values are generally less than 5%, all of which is considered acceptable.

4.2 Age-Temperature (A-T) plots

The MET-pIRIR ages were derived from the equivalent dose and the dosimetry data (Table 1). These feldspar ages, together with the expected ages, are summarized in Table 3. It is noted that no residual ages has been corrected for our samples, because it was observed that the residual dose is only a few Gy for the high-temperature MET-pIRIR signals for the Luochuan loess (Fu et al., submitted). A straightforward comparison of MET-pIRIR ages to expected ages can be illustrated in A-T plots. Typical A-T plots from 4 samples with different ages are shown in Fig. 2. The expected ages are shown as shaded bands in Fig. 2. It is observed that the IRSL ages obtained at 50 °C are the lowest ones, which significantly underestimate the expected chronology. This can be explained as a result of anomalous fading. The ages tend to increase with the stimulation temperature and an age plateau can be reached at higher temperatures. For the youngest sample in Fig. 2, LC-096, the MET-pIRIR ages measured at 200°C and above are consistent with the expected ages (yellow shaded area). Similar results were also observed for the two younger samples, LC-019 and LC-054 (Table 3). However, for older samples in Fig. 2, LC-133, LC-170 and LC-230, the MET-pIRIR ages measured at 200°C were underestimated, and only the 250 and 300 °C signals gave consistent ages with the expected ages (Fig. 2). This result suggests that the natural luminescence of the MET-pIRIR measured at 200°C probably suffered from anomalous fading, although in a small extent. This was not detectable for the relatively young samples (<130 ka for our samples). Such a small anomalous fading rate became important for older samples, resulting in an age underestimation. Therefore, the results suggest that the MET-pIRIR

175 ages obtained using temperature at 200°C and above are more reliable for older samples (>130 ka)
176 than the 200 °C MET-pIRIR signals. However, for younger samples, the 200 °C MET-pIRIR signals
177 can still be used for age determination, given its lower residual ages compared to the signals at higher
178 temperatures (Li and Li, 2011). Hence, the presence of an age plateau in the A-T plot is an important
179 criterion for the selection of appropriate MET-pIRIR temperatures.

180

181 **4.3 Natural dose response curves**

182 Based on expected ages and the dose rates, one can calculate the expected paleodose for each
183 sample (Table 3). It is thus possible to reconstruct the natural dose response curve (N-DRC) for the
184 loess sample in Luochuan section. In Fig. 3, the sensitivity-corrected natural MET-pIRIR signals
185 (L_n/T_n) at different temperatures from different samples were plotted against the corresponding
186 expected paleodoses. The smooth growth of the natural signal intensities for different samples at
187 different depth and ages suggested that these samples have a similar dose response behaviour in nature.
188 Different MET-pIRIR signals at different temperatures have different sensitivity-corrected intensities,
189 but all the N-DRCs appear to be able to grow up to a dose level around ~1000 Gy. It is interesting to
190 note that, if these natural DRCs are fitted with single exponential saturation functions (not shown in
191 Fig. 3), the values of the natural saturation doses (D_0) are 421, 338, 341, 324, 307 and 250 Gy for the
192 MET-pIRIR signals at 50, 100, 150, 200, 250 and 300 °C, respectively. These values are identical to
193 those obtained for laboratory DRCs shown in Fig. 1. The results indicate that the same origins of traps
194 were involved for both the natural signals and laboratory signals. However, the different saturation
195 dose levels for different MET-pIRIR signals at different temperatures indicate that these signals are
196 probably involved from different groups of traps.

197 For comparison, the laboratory DRCs for different MET-pIRIR signals shown in Fig. 1 are
198 also shown (note that the laboratory DRCs shown in Fig. 3 are the best fitting curves from Fig. 1). It is
199 shown from Fig. 3(a) that the N-DRC for the 50 °C IRSL signal is considerably below the laboratory
200 DRC. If the natural intensity is projected onto the laboratory DRC, significant dose underestimation

will be resulted. In addition, older samples with larger paleodoses yield increasing underestimations, i.e. the dose (or age) underestimation increase from ~22% for the youngest sample LC-019 to ~55% for the sample LC-270. This result clearly supports the dose-dependent effect of the anomalous fading rate in nature (Li and Li, 2008). A similar pattern was observed for the 100 °C MET-pIRIR signal (Fig. 3(b)), but a lower underestimation was observed, i.e. the N-DRC is more close to the laboratory DRC when compared to the 50 °C IRSL signal, suggesting that there is a lower anomalous fading for the 100 °C MET-pIRIR signal. This is consistent with the anomalous fading rate test in Li and Li (2011) showing that there is a lower fading rate for the higher MET-pIRIR temperatures. A dose underestimation ranging from ~9% to ~50% from young samples to old samples were still observed for the 100 °C MET-pIRIR signal. For the 150 °C MET-pIRIR signal (Fig. 3(c)), the N-DRC is even more close to the laboratory DRC. It is interesting to note that the natural intensity from the youngest sample LC-019 is consistent with laboratory DRC, indicating a negligible underestimation and anomalous fading for this sample. For older samples, dose underestimation ranging from ~18% to ~40% was still observed.

For sediments younger than 130 ka it was previously suggested that MET-pIRIR stimulated at 200°C was sufficient to yield accurate ages, mostly derived from quartz OSL ages, from different regions of China (Li and Li, 2011). This is consistent with the results in Fig. 3(d), which shows that the N-DRC is consistent with the laboratory DRC for samples with paleodose less than ~500 Gy (equivalent to ~140 ka). However, it is important to note that the 200 °C MET-pIRIR signal do get age underestimation for natural dose above ~500 Gy. For these older samples with paleodose larger than 500 Gy, the natural luminescence intensities are slightly below the laboratory DRC. A small underestimation in the signal intensity can cause a significant underestimation in age (or dose), because the dose are located in the saturation part of the DRC. Therefore, we conclude that a considerable age underestimation may be caused for older samples with higher natural doses (e.g. >~500 Gy), even though a small anomalous fading rate (e.g. <1%decade) was observed in

laboratory fading test. It is thus required to use higher MET-pIRIR temperatures to achieve non-fading components for these samples.

Despite of the underestimation observed for the MET-pIRIR signals at low temperatures (<200 °C), the N-DRCs for the MET-pIRIR signals at 250 and 300 °C show an excellent agreement with the laboratory DRCs for all samples investigated (Fig. 3(e) and Fig. 3(f)), indicating that a non-fading component can be achieved using a MET-pIRIR temperature at 250 °C and above. This can be further supported by measuring the natural intensities of the oldest sample from the ninth loess layer (L9), LC-626, which is expected to have received a natural dose of ~3000 Gy (equivalent to ~900 ka). Since the paleodose of LC-626 has far exceeded the natural saturation dose level (~1000 Gy), it can be treated as an infinite old sample whose luminescence attained an equilibrium state with the dose rate. The natural intensity of this sample should be consistent with the laboratory saturation level if there is no fading in nature and the signals are thermally stable. Our recent results (Li and Li, 2011; Li and Li, submitted) on the thermal stability of the MET-pIRIR signals indicated that these signals are thermally stable up to several million years. Therefore, anomalous fading would be expected to have occurred if the natural luminescence intensity from the field-saturated sample is lower than the saturation level of the laboratory-irradiated sample.

The natural MET-pIRIR intensities at different temperatures for LC-626 were shown as shaded area in Fig. 3. Note that the shaded area shows the 1σ standard deviation. It is clearly shown that the natural intensities of LC-626 are consistent with those of samples with paleodose larger than ~1000 Gy, indicating that these samples have also reached at field saturation. The field saturation levels are below the laboratory saturation level for the MET-pIRIR signals at 50, 100, 150 and 200 °C, indicating that there were anomalous fading in nature for these signals. The difference between the field and laboratory saturation levels decreased as the stimulation temperature increased. This is expected because there is a lower anomalous fading rate for the signals at higher temperature. It is interesting to note that the field saturation levels agree very well with the laboratory saturation level

for the MET-pIRIR signals at 250 and 300 °C, confirming that the signals measured at 250 °C and above suffer negligible anomalous fading.

4.4 Dating results for Luochuan section

The protocol shown in Table 2 has been applied to all samples and the MET-pIRIR ages were summarized in Table 3. All the ages were obtained from measurements of 4-6 aliquots. These ages, together with the stratigraphic column, are plotted against sampling depth in Fig. 4. The independent ages of the loess/paleosol (L/S) boundaries from Ding et al. (2002) are also shown. These age constrains were used for generating an age-depth curve (shown as full curve in Fig. 4), using linear interpolation of the sampling depth between the upper and lower boundaries of the loess or paleosol layers.

In Fig. 4, it is shown that the IRSL ages obtained at 50 °C are all underestimated. The ages tend to increase as the stimulation temperature increased. There is a good agreement between the MET-pIRIR 200°C ages and the expected ages for the samples younger than ~130 ka (from L1 and S1). The MET-pIRIR 200°C underestimated the expected ages for older samples. For the 250 and 300 °C signals, the obtained ages are consistent with expected ages up to ~300 ka (equivalent to the lower part of L3). This suggests that the MET-pIRIR signals at 250 and 300 °C suffers from negligible anomalous fading and can be used to evaluate the K-feldspar age beyond 130 ka without fading correction.

For the sample (LC-270) older than 300 ka, the uncertainty of the ages of the MET-pIRIR signals at 250 and 300 °C become extremely large, which is mainly due to the saturation of the MET-pIRIR signals at 250 and 300 °C (see Fig. 3). Therefore, we conclude that the MET-pIRIR protocol has an age limit of ~300 ka (equivalent to a dose limit of ~900 Gy) for the Chinese loess.

In summary, based on the dating results, we suggest to use the MET-pIRIR 250 ºC ages as the best age estimates for samples above S1 (<130 ka), and to used the average of the 250 and 300 ºC ages as the best age estimates for older samples (shown in the last column of Table 3).

9. Conclusions

The MET-pIRIR signals protocol of measuring the IRSL signal from K-feldspars by progressively increasing the stimulation temperature from 50 to 300°C in step of 50°C can be successfully applied to the loess/paleosol units from L1 to L3 at the Luochuan section. When compared to the expected ages based on stratigraphic correlation, the IRSL obtained at 50°C has the largest underestimation in age. The extent of age underestimation decreases as the stimulation temperature increases. The ages for the 200°C MET-pIRIR signal are consistent with expected age for young samples (<130 ka), but are underestimated for older samples (>130 ka). Negligible anomalous fading was observed for the MET-pIRIR signals obtained at 250 and 300°C, which is supported by the age-temperature (A-T) plots showing age plateau above 250°C. The 250 and 300 °C MET-pIRIR signals can give reliable age estimation for the Chinese loess up to ~300 ka.

Acknowledgements

Dr. Xulong Wang is appreciated for his help in sampling for this study. The study is financially supported by grants to SHL from the Research Grant Council of the HKSAR, China (Project No. 7035/06P, 7035/07P and 7028/08P).

References

Aitken, M.J., 1985. *Thermoluminescence dating*. Academic press, London.

296 An, Z.H., Kukla, G.J., Porter, S.C., Xiao, J.L., 1991. Magnetic-Susceptibility Evidence of Monsoon
297 Variation on the Loess Plateau of Central China during the Last 130,000 Years. *Quaternary Research*
298 **36**, 29-36.
299 Bøtter-Jensen, L., Andersen, C.E., Duller, G.A.T., Murray, A.S., 2003. Developments in radiation,
300 stimulation and observation facilities in luminescence measurements. *Radiat Meas* **37**, 535-541.
301 Bøtter-Jensen, L., Bulur, E., Duller, G.A.T., Murray, A.S., 2000. Advances in luminescence
302 instrument systems. *Radiat Meas* **32**, 523-528.
303 Buylaert, J.P., Murray, A.S., Thomsen, K.J., Jain, M., 2009. Testing the potential of an elevated
304 temperature IRSL signal from K-feldspar. *Radiat Meas* **44**, 560-565.
305 Buylaert, J.P., Vandenberghe, D., Murray, A.S., Huot, S., De Corte, F., Van den Haute, P., 2007.
306 Luminescence dating of old (> 70 ka) Chinese loess: A comparison of single-aliquot OSL and IRSL
307 techniques. *Quaternary Geochronology* **2**, 9-14.
308 Ding, Z.L., Derbyshire, E., Yang, S.L., Yu, Z.W., Xiong, S.F., Liu, T.S., 2002. Stacked 2.6-Ma grain
309 size record from the Chinese loess based on five sections and correlation with the deep-sea delta O-18
310 record. *Paleoceanography* **17**, -.
311 Forman, S.L., 1991. Late Pleistocene Chronology of Loess Deposition near Luochuan, China.
312 *Quaternary Res* **36**, 19-28.
313 Frechen, M., 1999. Luminescence dating of loessic sediments from the Loess plateau, China.
314 *Geologische Rundschau* **87**, 675-684.
315 Huntley, D.J., Lamothe, M., 2001. Ubiquity of anomalous fading in K-feldspars and the measurement
316 and correction for it in optical dating. *Canadian Journal of Earth Sciences* **38**, 1093-1106.
317 Huntley, D.J., Lian, O.B., 2006. Some observations on tunnelling of trapped electrons in feldspars and
318 their implications for optical dating. *Quaternary Science Reviews* **25**, 2503-2512.
319 Imbrie, J., Haye, J.D., Martinson, D.B., McIntyre, A., Mix, A.C., Morley, J.J., Pisias, N.G., Prell,
320 W.L., Shackleton, N.J., 1984. The orbital theory of Pleistocene climate: support from a revised
321 chronology of the marine $\delta^{18}O$ record. , in: Berger, A.I., J., Hays, G., Kukla, G., Saltzman, B. (Ed.),
322 Milankovitch and Climate, Reidel, Dordrecht, pp. 269-305.
323 Lai, Z.P., 2010. Chronology and the upper dating limit for loess samples from Luochuan section in the
324 Chinese Loess Plateau using quartz OSL SAR protocol. *Journal of Asian Earth Sciences* **37**, 176-185.
325 Lai, Z.P., Zhang, W.G., Chen, X., Jia, Y.L., Liu, X.J., Fan, Q.S., Long, H., 2010. OSL chronology of
326 loess deposits in East China and its implications for East Asian monsoon history. *Quaternary*
327 *Geochronology* **5**, 154-158.
328 Lamothe, M., Auclair, M., 1999. A solution to anomalous fading and age shortfalls in optical dating of
329 feldspar minerals. *Earth and Planetary Science Letters* **171**, 319-323.
330 Li, B., Li, S.H., 2008. Investigations of the dose-dependent anomalous fading rate of feldspar from
331 sediments. *Journal of Physics D-Applied Physics* **41**, 225502.

Li, B., Li, S.H., 2011. Luminescence dating of K-feldspar from sediments: A protocol without anomalous fading correction. *Quaternary Geochronology* **6**, 468-479.

Li, B., Li, S.H. On the thermal stability and kinetics of the infrared stimulated luminescence from K-feldspar. *Journal of Luminescence*, Submitted.

Li, B., Li, S.H., Wintle, A.G., Zhao, H., 2007. Isochron measurements of naturally irradiated K-feldspar grains. *Radiat Meas* **42**, 1315-1327.

Liu, T.S., 1985. *Loess and the environment*. China Ocean Press, Beijing.

Lu, Y.C., Prescott, J.R., Robertson, G.B., Hutton, J.T., 1987. Thermo-Luminescence Dating of the Malan Loess at Zhaitang, China. *Geology* **15**, 603-605.

Lu, Y.C., Wang, X.L., Wintle, A.G., 2007. A new OSL chronology for dust accumulation in the last 130,000 yr for the Chinese Loess Plateau. *Quaternary Res* **67**, 152-160.

Porter, S.C., An, Z.S., 1995. Correlation between Climate Events in the North-Atlantic and China during Last Glaciation. *Nature* **375**, 305-308.

Prescott, J.R., Hutton, J.T., 1994. Cosmic-Ray Contributions to Dose-Rates for Luminescence and Esr Dating - Large Depths and Long-Term Time Variations. *Radiat Meas* **23**, 497-500.

Thomsen, K.J., Murray, A.S., Jain, M., Botter-Jensen, L., 2008. Laboratory fading rates of various luminescence signals from feldspar-rich sediment extracts. *Radiat Meas* **43**, 1474-1486.

Wang, X.L., Lu, Y.C., Wintle, A.G., 2006. Recuperated OSL dating of fine-grained quartz in Chinese loess. *Quaternary Geochronology* **1**, 89-100.

Wintle, A.G., Murray, A.S., 2006. A review of quartz optically stimulated luminescence characteristics and their relevance in single-aliquot regeneration dating protocols. *Radiat Meas* **41**, 369-391.

Zhou, L.P., Shackleton, N.J., 2001. Photon-stimulated luminescence of quartz from loess and effects of sensitivity change on palaeodose determination. *Quaternary Science Reviews* **20**, 853-857.

Figure captions

Figure 1: The dose response curves for the MET-pIRIR signals at different temperatures. The data points are the average of the data sets obtained from five samples, LC-096, LC-120, LC-150, LC-170 and LC-250. The test dose used is 54Gy.

Figure 2: Typical age-temperature (A-T) plots for samples LC-096, LC-133, LC-170 and LC-230 obtained using the protocol of Table 2. The yellow shaded area in each plot shows the expected age (see Table 3 for values).

Figure 3: The sensitivity-corrected natural MET-pIRIR signals (L_n/T_n) at different temperatures from different samples plotted against the corresponding expected paleodoses (values from Table 3). The best fitting curves of the laboratory DRCs from Fig. 1 are also shown as full curves. The horizontal dashed line and shaded area shows the natural MET-pIRIR intensities for sample LC-626, which has reached field saturation level (see text). Note that the shaded area shows the 1σ standard deviation.

Figure 4: The MET-pIRIR ages (data points) (values in Table 3) and expected ages (full curve) plotted against sampling depth. The paleosol/loess units are shown as stratigraphic column on the right. The independent ages of the loess/paleosol (L/S) boundaries from Ding et al. (2002) are also shown beside the stratigraphic column. The expected ages are based on linear interpolation of the sampling depth between the upper and lower boundaries of the loess or paleosol layer from which the sample was taken.

Figure 1

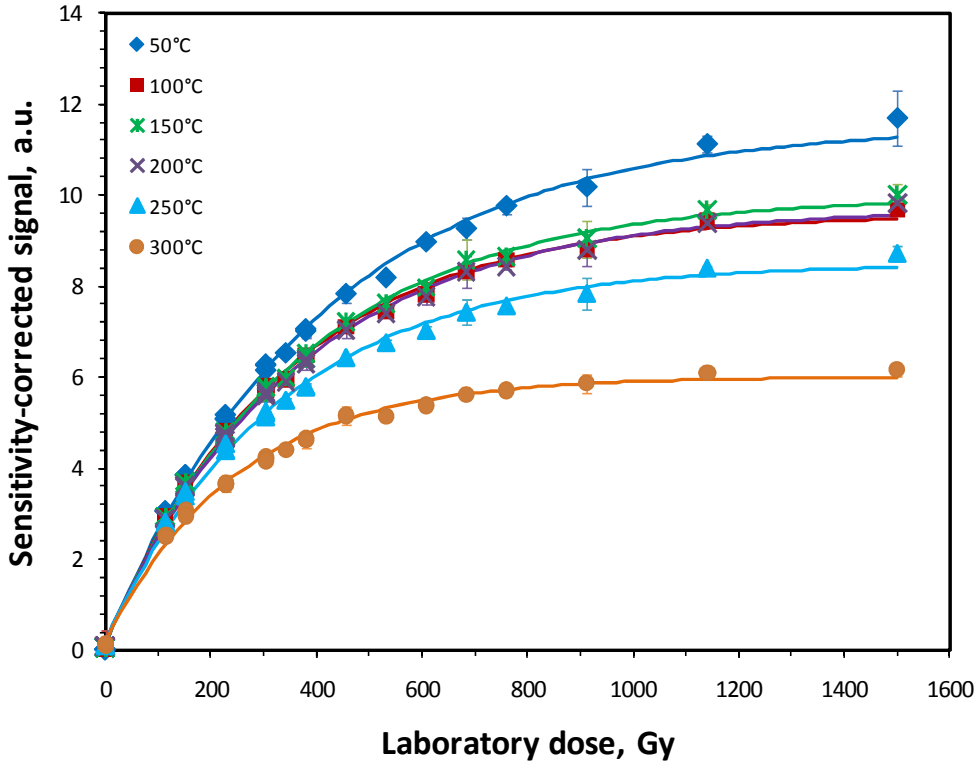
Sensitivity-corrected signal, a.u.
Laboratory dose, Gy
50°C
100°C
150°C
200°C
250°C
300°C
0
2
4
6
8
10
12
14
0
200
400
600
800
1000
1200
1400
1600

Figure 2

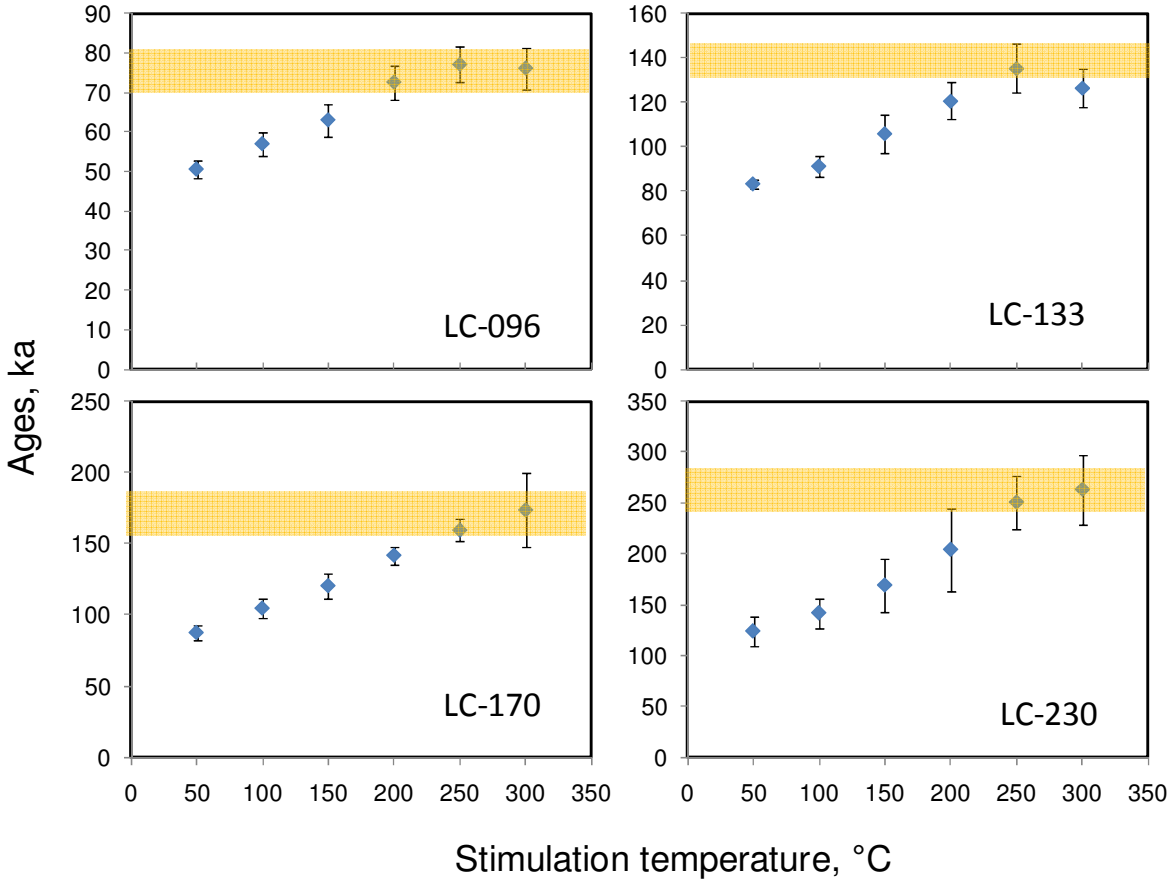

Figure 3

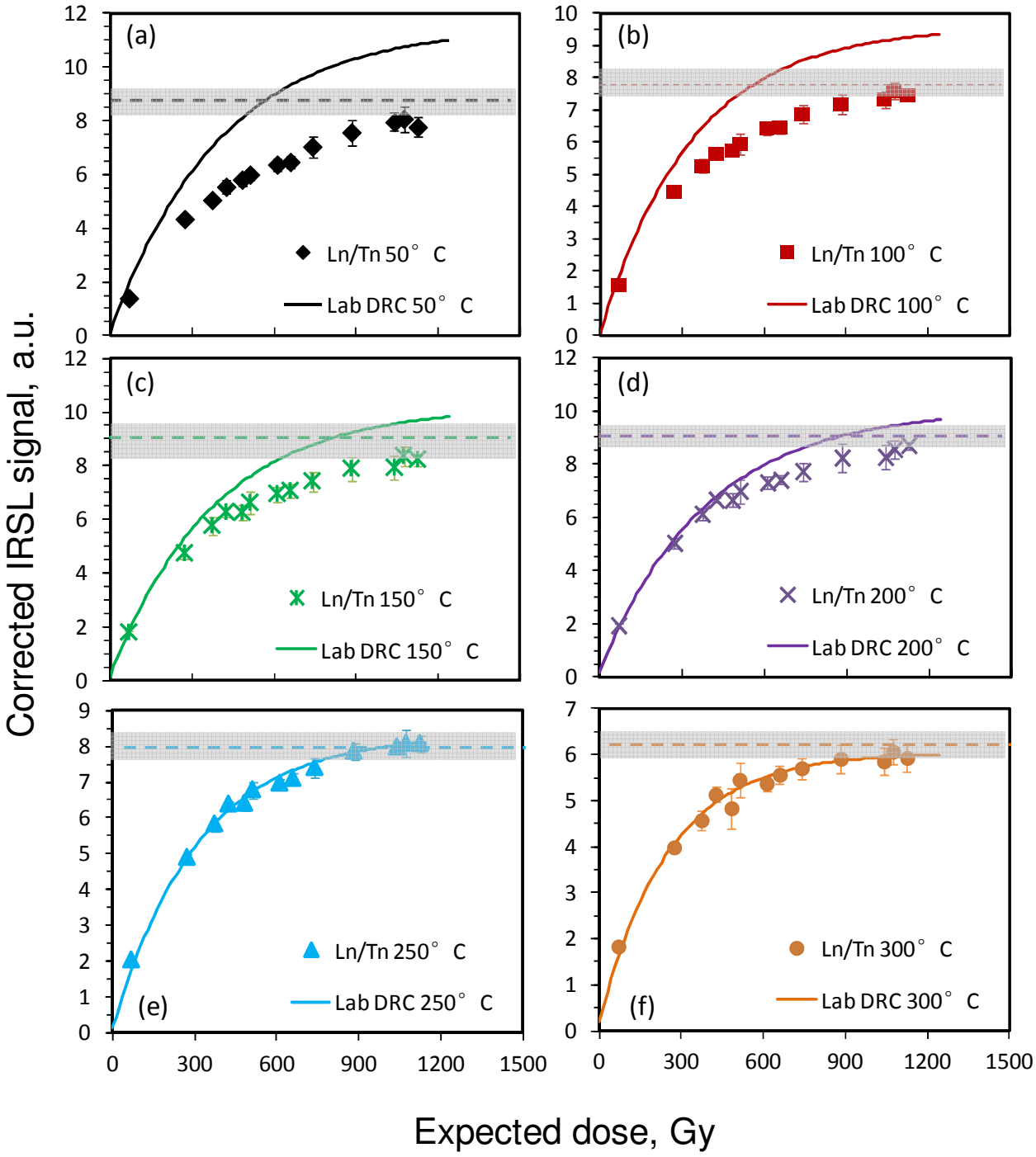
(a)
Ln/Tn 50° C
Lab DRC 50° C
(b)
Ln/Tn 100° C
Lab DRC 100° C
(c)
Ln/Tn 150° C
Lab DRC 150° C
(d)
Ln/Tn 200° C
Lab DRC 200° C
(e)
Ln/Tn 250° C
Lab DRC 250° C
(f)
Ln/Tn 300° C
Lab DRC 300° C
Corrected IRSL signal, a.u.
Expected dose, Gy

Figure 4

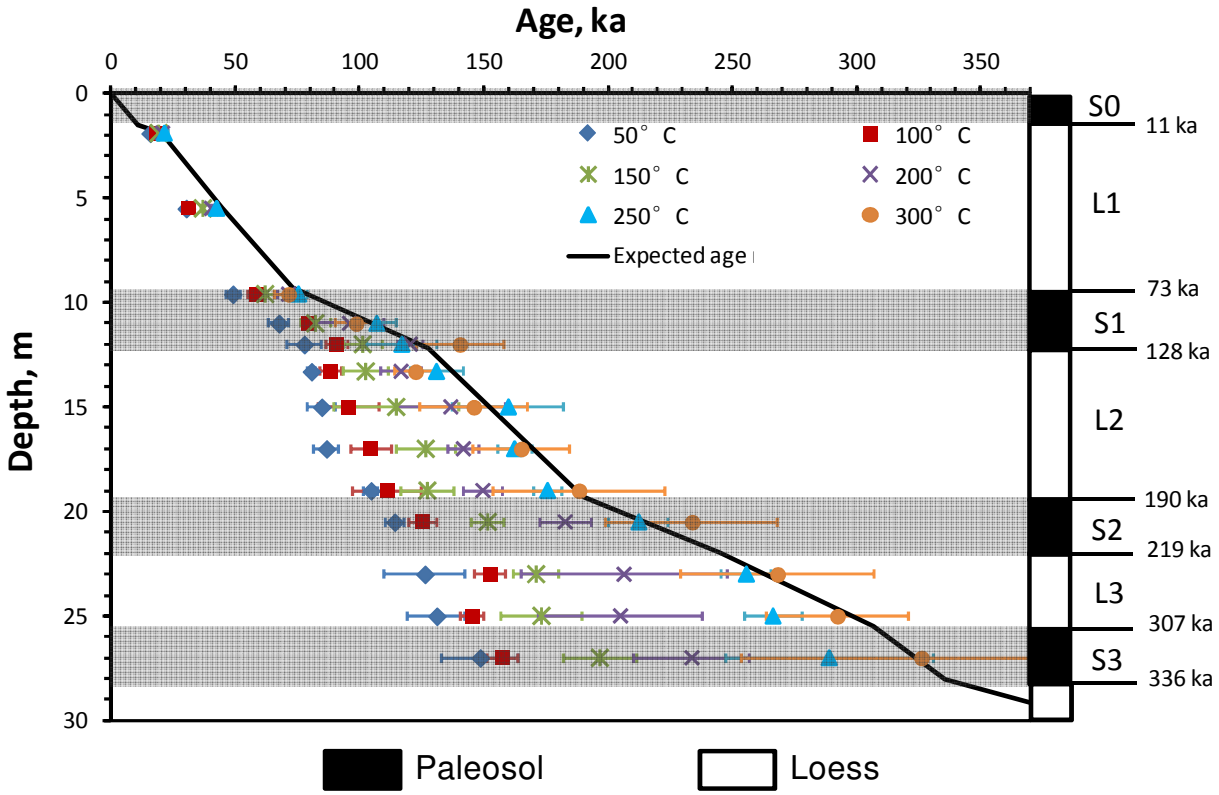
Age, ka
0
50
100
150
200
250
300
350
Depth, m
0
5
10
15
20
25
30
50° C
100° C
150° C
200° C
250° C
300° C
Expected age
S0
11 ka
L1
73 ka
S1
128 ka
L2
190 ka
S2
219 ka
L3
307 ka
S3
336 ka
Paleosol
Loess

Table 1: Summary of sammpling depth, stratigraphic unit and the dosimetry data for the samples.

Sample	Depth (m)	Unit	Grain size (μm)	K content (%)	Alpha count rate (cts/ks)	Water content (%)	Cosmic rays (Gy/ka)	Ext. dose rate (Gy/ka)	Int. dose rate [a] (Gy/ka)
LC-019	1.9	L1	63-90	1.70	11.38±0.22	15±5	0.17	3.1±0.1	0.36
LC-054	5.4		63-90	1.97	12.33±0.19	15±5	0.09	3.3±0.1	0.36
LC-096	9.6	S1	63-90	2.06	12.86±0.20	20±5	0.06	3.3±0.1	0.36
LC-110	11.0		63-90	1.98	12.66±0.19	20±5	0.05	3.2±0.1	0.36
LC-120	12.0		63-90	2.10	11.37±0.18	20±5	0.05	3.1±0.1	0.36
LC-133	13.3	L2	63-90	1.90	11.65±0.22	15±5	0.04	3.2±0.1	0.36
LC-150	15.0		63-90	1.85	10.97±0.18	15±5	0.04	3.0±0.1	0.36
LC-170	17.0		63-90	2.00	11.77±0.25	15±5	0.03	3.2±0.1	0.36
LC-190	19.0		63-90	1.96	11.43±0.25	15±5	0.03	3.2±0.1	0.36
LC-205	20.5	S2	63-90	1.97	12.19±0.23	20±5	0.03	3.1±0.1	0.36
LC-230	23.0	L3	63-90	1.83	11.17±0.24	15±5	0.03	3.0±0.1	0.36
LC-250	25.0		63-90	1.93	11.46±0.20	15±5	0.02	3.1±0.1	0.36
LC-270	27.0	S3	63-90	1.90	11.54±0.20	20±5	0.02	3.0±0.1	0.36
LC-290	29.0	L4	63-90	1.89	11.77±0.20	15±5	0.01	3.1±0.1	0.36
LC-626	62.6	L9	63-90	-	-	-	-	-	-

Note: [a] The internal dose rate for K-feldspar used in age calculation was estimated by assuming K=13±1% and Rb=400±100 ppm (Li et al. 2008; Huntley and Baril, 1997; Zhao and Li, 2005; Huntley and Hancock, 2001).

Table 2: The single-aliquot regenerative-dose (SAR) protocol for multi-elevated-temperatures post-IR IRSL.

MET-pIRIR protocol		
Step	Treatment	Observed
1	Give regenerative dose, D_i [a]	
2	Preheat at 320°C for 60 s	
3	IRSL measurement at 50°C for 100 s	$L_{x(50)}$
4	IRSL measurement at 100°C for 100 s	$L_{x(100)}$
5	IRSL measurement at 150°C for 100 s	$L_{x(150)}$
6	IRSL measurement at 200°C for 100 s	$L_{x(200)}$
7	IRSL measurement at 250°C for 100 s	$L_{x(250)}$
8	IRSL measurement at 300°C for 100 s	$L_{x(300)}$
9	Give test dose, D_t	
10	Preheat at 320°C for 60 s	
11	IRSL measurement at 50°C for 100 s	$T_{x(50)}$
12	IRSL measurement at 100°C for 100 s	$T_{x(100)}$
13	IRSL measurement at 150°C for 100 s	$T_{x(150)}$
14	IRSL measurement at 200°C for 100 s	$T_{x(200)}$
15	IRSL measurement at 250°C for 100 s	$T_{x(250)}$
16	IRSL measurement at 300°C for 100 s	$T_{x(300)}$
17	IR bleaching at 325°C for 100 s	
18	Return to step 1	

[a] For the 'natural' sample, i= 0 and $D_0 = 0$. The whole sequence is repeated for several regenerative doses including a zero dose and a repeated dose.

Table 3. Summary of the samples used and their corresponding ages obtained using different signals.

Sample	Depth (m)	Unit	Expected age [a] (ka)	Paleodose [b] (ka)	K-feldspar MET-pIRIR ages (ka) [c]						KF ages (ka) [d]
					50°C	100°C	150°C	200°C	250°C	300°C	
LC-019	1.9	L1	20±3	69±10	15.7±0.4	18.4±0.4	19.2±0.4	20.8±0.6	21.5±1.8	-	21.5±1.8
LC-054	5.4		46±4	273±13	30.2±0.7	31.4±1.4	37.0±1	40.5±0.7	42.4±2.8	-	42.4±2.8
LC-096	9.6		75±5	374±18	49.0±2.8	58.6±3.7	62.1±3.9	71.5±4.3	75.5±3.7	71.4±5.5	75.5±3.7
LC-110	11.0	S1	105±5	425±18	67.5±3.9	79.2±1.5	82.3±6.0	96.0±13.5	107.0±7.9	98.6±8.5	107.0±7.9
LC-120	12.0		124±5	483±17	77.7±6.8	90.9±4.4	101.4±7.6	120.5±5.1	117.1±14.3	140.4±17.5	117.1±14.
LC-133	13.3		138±5	512±34	80.6±1.8	88.3±4.5	102.6±8.9	116.8±8.0	131.1±10.8	122.5±8.5	127±7
LC-150	15.0	L2	152±10	612±35	84.8±5.8	95.6±12.2	114.9±25.0	136.8±22.2	160.0±22.4	146.0±21.5	153±16
LC-170	17.0		170±10	660±36	86.7±5.1	104.6±8.2	126.7±11.9	141.9±6.2	162.5±6.8	165.0±19.3	164±10
LC-190	19.0		187±10	740±35	104.6±2.9	111.3±13.8	127.4±10.7	149.7±7.6	175.8±5.5	188.3±34.6	182±18
LC-205	20.5	S2	214±10	883±35	114.1±3.7	125.4±5.8	151.6±6.4	182.8±10.4	212.5±11.9	233.8±34.6	223±18
LC-230	23.0	L3	263±10	1041±34	126.3±16.5	152.7±6.2	171.1±9.0	206.5±41.3	255.7±10.0	268.2±38.8	262±20
LC-250	25.0		298±15	1074±35	131.1±11.6	145.4±4.7	173.3±16.1	205.1±32.9	266.5±11.6	292.3±28.7	279±15
LC-270	27.0	S3	324±15	1125±50	148.5±15.2	157.8±6.4	196.8±14.8	233.8±23.3	289.1±41.7	326.1±72.5	308±42
LC-290	29.0	L4	340±15	1190±33	-	-	-	-	-	-	-
LC-626	62.6	L9	900	3000	-	-	-	-	-	-	-

Note: [a] The expected age of sample LC-054 is based on OSL dating fine-grain quartz (see Fu et al., this issue). For other samples, all expected ages are based on stratigraphic ages (see text for detailed description of the expected age model).

[b] The expected paleodoses are calculated using the expected ages and the dose rates provided in Table 2.

[c] The MET-pIRIR ages for LC-019 and LC-054 are based on the original protocol of Li and Li (2011), in which the stimulation temperatures of 50-250°C were used. The MET-pIRIR ages for LC-290 and LC-626 cannot be obtained because the saturation of the natural signals.

[d] The KF ages in the last column are the best age estimates for the samples. For samples above S1 (<130 ka), the MET-pIRIR 250 ºC ages were used, and for older samples the average of the 250 and 300 ºC ages were used.